Tumor Regression by Targeted Gene Delivery to the Neovasculature

John D. Hood,[1] Mark Bednarski,[2] Ricardo Frausto,[1] Samira Guccione,[2] Ralph A. Reisfeld,[1] Rong Xiang,[1] David A. Cheresh[1]*

Efforts to influence the biology of blood vessels by gene delivery have been hampered by a lack of targeting vectors specific for endothelial cells in diseased tissues. Here we show that a cationic nanoparticle (NP) coupled to an integrin αvβ3–targeting ligand can deliver genes selectively to angiogenic blood vessels in tumor-bearing mice. The therapeutic efficacy of this approach was tested by generating NPs conjugated to a mutant *Raf* gene, *ATP$^{\mu}$-Raf*, which blocks endothelial signaling and angiogenesis in response to multiple growth factors. Systemic injection of the NP into mice resulted in apoptosis of the tumor-associated endothelium, ultimately leading to tumor cell apoptosis and sustained regression of established primary and metastatic tumors.

Vascular targeting offers therapeutic promise for the delivery of drugs (*1*) and radionuclides (*2*). Moreover, targeting of genes to specific blood vessels may provide complementary approaches to disrupt or induce the growth of new blood vessels in various disease states. Viral vectors (*3*), liposomes (*4*), and naked DNA (*5*, *6*) have been used for delivery of therapeutic genes to vascular tissue, but none of these approaches are specific for endothelial cells.

During vascular remodeling and angiogenesis, endothelial cells show increased expression of several cell surface molecules that potentiate cell invasion and proliferation (*7*, *8*). One such molecule is the integrin αvβ3, which plays a key role in endothelial cell survival during angiogenesis in vivo (*9*). In addition to its role in cell matrix recognition, αvβ3 may be of particular use in gene delivery strategies, because this receptor potentiates the internalization of foot-and-mouth disease virus (*10*), rotavirus (*11*), and adenovirus (*12*), thereby facilitating gene transfer. The fact that αvβ3 is preferentially expressed in angiogenic endothelium and contributes to viral internalization prompted us to consider it as an endothelial cell target for nonviral gene delivery.

We synthesized a cationic polymerized lipid-based NP that was covalently coupled to a small organic αvβ3 ligand (αvβ3-NP) (*13*) (Fig. 1). The αvβ3-binding ligand was selective for αvβ3 in both receptor-binding studies and cell adhesion experiments, with a mean inhibitory concentration (IC_{50}) of 0.04 μM for purified αvβ3 as compared to an IC_{50} of 5.5 μM for αvβ5 and 2.1 μM for αIIbβ3. In cell adhesion experiments, this compound was 100 times more potent at disrupting αvβ3-mediated as αvβ5-mediated cell attachment to vitronectin (0.33 μM versus 30 μM, respectively) (*13*).

To establish that αvβ3-NP could selectively deliver genes to αvβ3-bearing cells, we coupled αvβ3-NP to the gene encoding green fluorescence protein (GFP) and allowed the particles to interact with cultured human melanoma cells expressing αvβ3 (M21) or lacking αvβ3 (M21-L) (*14*). The αvβ3-NP selectively transduced GFP into M21 cells but not M21-L cells (Fig. 2A). A nontargeted NP (nt-NP), in which the integrin antagonist was replaced by an arginine residue to mimic the zwitterionic surface charge of the αvβ3-targeting ligand, showed no gene delivery to either cell type. A 20-fold molar excess of the soluble αvβ3 ligand completely abolished gene delivery to M21 cells, further demonstrating that the selective delivery of the gene is integrin αvβ3-dependent (Fig. 2A).

To determine whether the αvβ3-NP could deliver genes to angiogenic tumor-associated blood vessels, we injected αvβ3-NP or nt-NP complexed with the gene encoding firefly luciferase into the tail vein of mice bearing αvβ3-negative M21-L melanomas. After 24 hours, maximal luciferase activity was detected in tumors after injection of NP coupled to 25 μg of luciferase (Fig. 2B inset). At this dose, minimal luciferase was detected in the lung and heart (Fig. 2B), and no detectable expression was found in the liver, brain, kidney, skeletal muscle, spleen, and bladder. Tumor-specific luciferase expression was completely blocked when mice were coinjected with a 20-fold molar excess of the soluble αvβ3-targeting ligand (Fig. 2B).

Components of the Ras-Raf-MEK-ERK pathway appear to play an important role in neovascularization, because blockade of this pathway suppresses angiogenesis in vivo (*15*). We focused on a mutant form of *Raf-1* that fails to bind ATP (ATP$^{\mu}$-Raf) (*16*) and blocks endothelial cell Raf activity in cultured endothelial cells (*13*). This mutant also blocks angiogenesis on the chick chorioallantoic membrane in response to basic fibroblast growth factor (bFGF) or vascular endothelial cell growth factor (VEGF) (*13*). In fact, mice lacking *Raf-1* die early in development with high levels of cellular apoptosis and vascular defects in the yolk sac and placenta (*17*).

To validate the vascular targeting capacity of this particle and to establish a role for *Raf-1* in angiogenesis, we coupled a cDNA encoding ATP$^{\mu}$-Raf tagged with the FLAG epitope to the αvβ3-NP [αvβ3-NP/Raf(–)]. M21-L melanomas, implanted subcutaneously, were allowed to grow for 9 days, at which time they reached a size of ~400 mm^3. We injected tumor-bearing mice intravenously (i.v.) with the αvβ3-NP/Raf(–). After 24 or 72 hours we removed the tumors and costained them with vascular endothelial (VE) cell–cadherin–specific antibody to identify blood vessels and a FLAG-specific antibody to detect gene expression. We also evaluated the tumors for terminal deoxynucleotidyl transferase-mediated deoxyuridine triphosphate nick-end labeling (TUNEL) staining, which marks apoptotic cells, because suppression of Raf activity has been reported to promote apoptosis (*18*). Twenty-four hours after the injection of αvβ3-NP/Raf(–), TUNEL-positive cells were detected only among the vessels that had been transduced (FLAG-tagged cells) (Fig. 3A). To assess the impact of ATP$^{\mu}$-Raf on tumor cell viability, we stained cryosections taken from tumors 72 hours after treatment and examined them at low magnification (100×) to evaluate both blood vessels and surrounding tumor parenchyma. In addition to the apoptosis among the blood vessels (VE-cadherin–positive cells), there were concentric rings of apoptosis (TUNEL-positive cells) among the tumor cells proximal to each apoptotic vessel (Fig. 3B). Accordingly, hematoxylin and eosin revealed extensive tumor necrosis (Fig. 3C).

To further test the therapeutic efficacy of this treatment, we randomly sorted mice bearing established 400-mm^3 M21-L tumors into four groups and treated each group with a single tail vein injection of phosphate-buffered saline (PBS), as a control; nt-NP/Raf(–); or αvβ3-NP/Raf(–). The fourth group was coinjected with αvβ3-NP/Raf(–) plus a 20-fold molar excess of the soluble αvβ3-targeting ligand. Mice injected with PBS or nt-NP/Raf(–) formed large tumors (1200 mm^3) and, consequently, were eu-

[1]Department of Immunology, The Scripps Research Institute, 10550 North Torrey Pines Road, La Jolla, CA 92037, USA. [2]Lucas Magnetic Resonance Spectroscopy Research Center, Stanford School of Medicine, 1201 Welch Road, Stanford, CA 94305, USA.

*To whom correspondence should be addressed. E-mail: cheresh@scripps.edu

thanized on day 25 (Fig. 4A). In contrast, mice injected with αvβ3-NP/Raf(–) displayed rapid tumor regression (Fig. 4A). Six days after treatment, four of six mice showed no evidence of tumors, and the two others showed a >95% reduction in tumor mass and a >75% suppression of blood vessel density (Fig. 4C). These tumor regressions were sustained for >250 days. Injection of excess soluble αvβ3 ligand, though slightly suppressive of tumor growth on its own, completely abolished the antitumor activity of αvβ3-NP/Raf(–) (Fig. 4A). These findings demonstrate that αvβ3-targeted delivery of ATPμS-Raf to blood vessels causes tumor regression because of its ability to promote

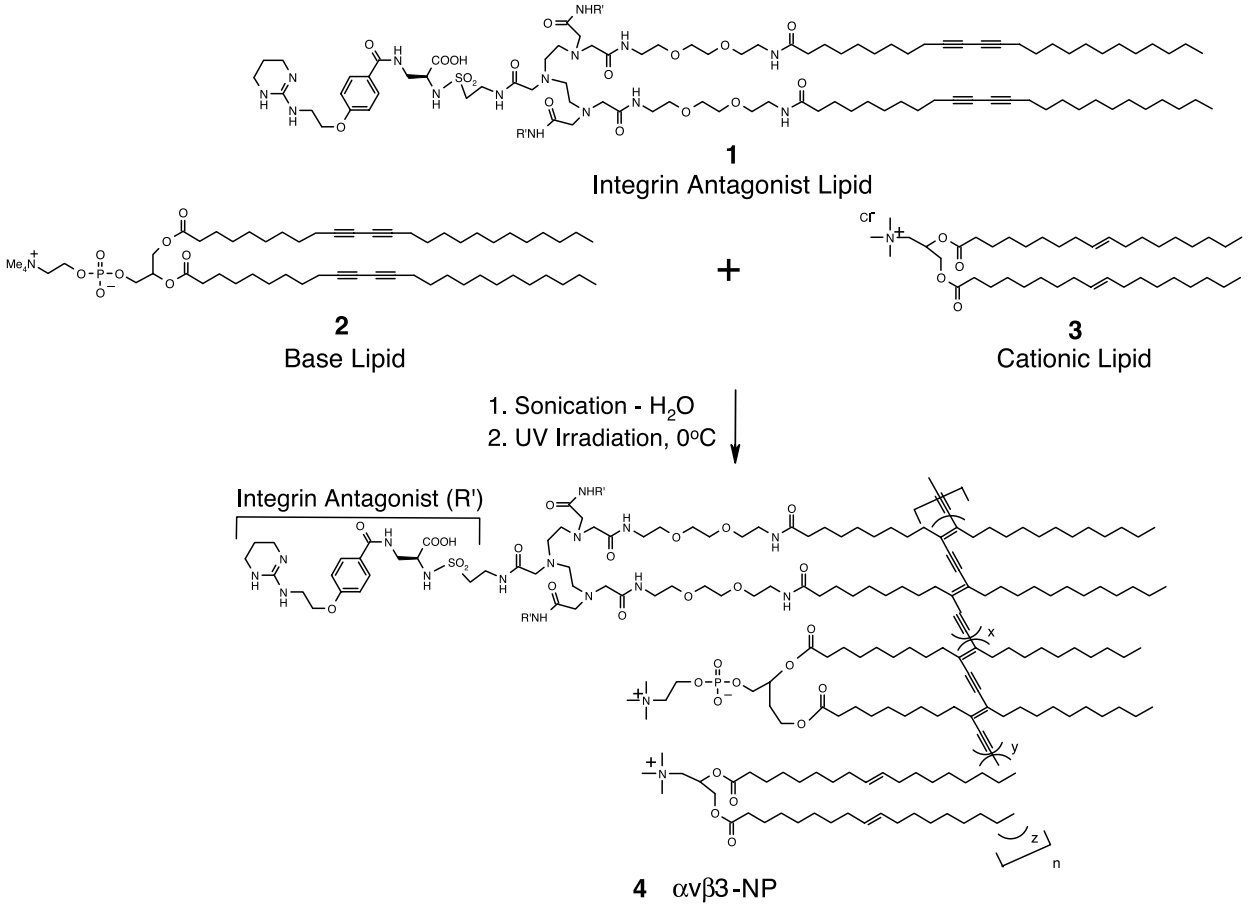

Fig. 1. Schematic diagram outlining the formation of the NPs by self-assembly and polymerization of the appropriate lipids. The trivalent lipid-integrin antagonist **1** was combined with diacetylene phospholipid **2** in a chloroform solution (*13*, *20*), to which the cationic lipid **3** was added to vary the surface charge. The surface density of the integrin antagonist on theNPs was set at 10 mole percent of the concentration of compound **2**. The mean diameter of the NPs was between 40 and 50 nm, as determined by dynamic light scattering, and the zeta potential was approximately +35 for the NPs used here. The NPs were stable for months without important changes in their physical and biological properties when formulated for use in vivo.

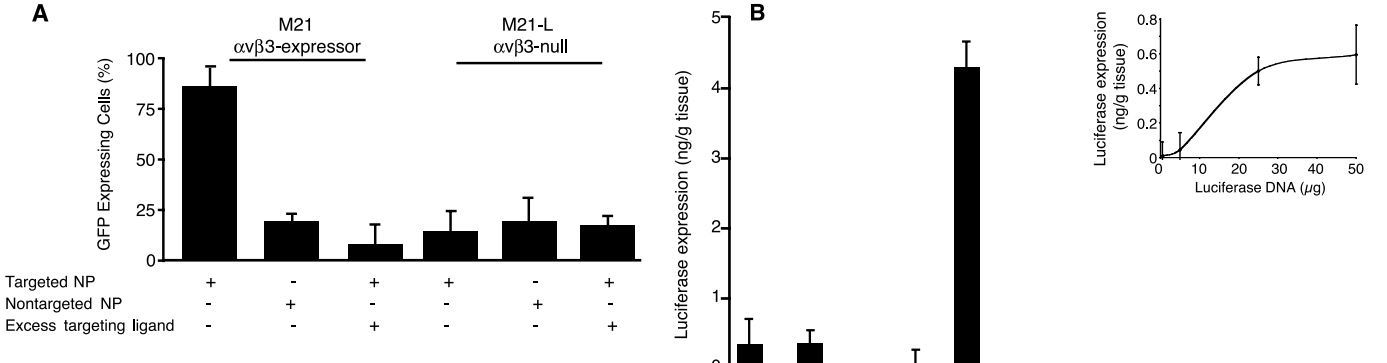

Fig. 2. αvβ3-NP–mediated gene delivery to αvβ3-bearing cells in vitro and in vivo. (**A**) GFP gene transfer mediated by αvβ3-NP to M21 or M21-L human melanoma cells was evaluated (*21*). (**B**) Athymic WEHI mice were subcutaneously injected with M21-L cells (5×10^6), and tumors were allowed to grow to ~100 mm^3. Mice were then injected i.v. with 450 nmoles of NP electrostatically coupled to 25 μg (*13*) of plasmid expressing firefly luciferase. One group also received a coinjection of 20-fold molar excess of the soluble αvβ3-targeting ligand. After 24 hours, mice were killed, tissues were surgically removed, and luciferase activity was quantified. (**Inset**) Luciferase expression as a function of DNA dose injected. Each bar represents the mean ± SD of five replicates.

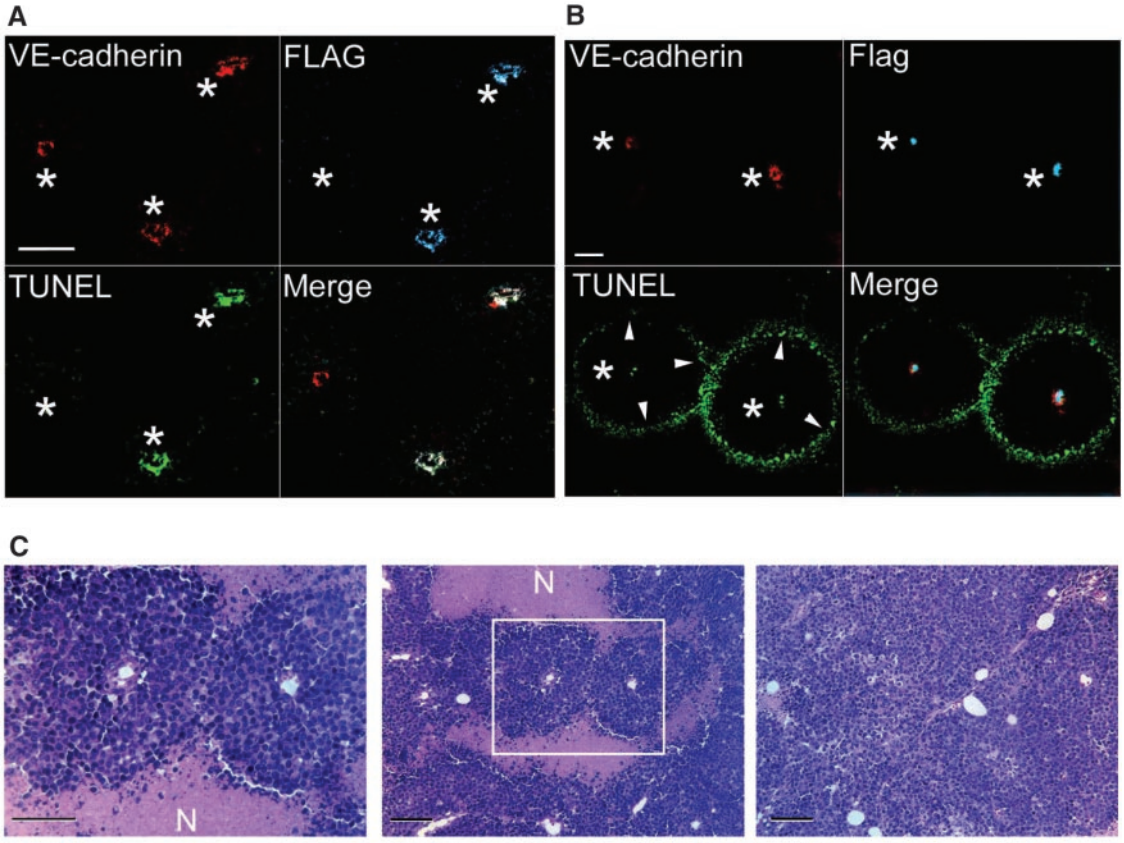

Fig. 3. Delivery of ATP$^{\mu}$-Raf to tumor-associated blood vessels causes endothelial and tumor cell apoptosis. Athymic WEHI mice were subcutaneously implanted with M21-L melanoma, and tumors were allowed to grow to ~400 mm^3. Mice were then given a single intravenous injection of αvβ3/NP-Raf(–). Control animals were injected with the αvβ3-NP coupled to a vector lacking the *Raf* gene (shuttle vector). After 24 or 72 hours, mice were killed, and their tumors were resected, fixed, sectioned, and stained (*13*). (**A**) Tumors harvested 24 hours after treatment were immunostained for VE-cadherin (endothelial cells), FLAG (gene expression), and TUNEL (apoptosis) (*22*). Bar, 50 μm. Asterisks, blood vessels. (**B**) Tumors harvested 72 hours after treatment were stained as above. Bar and asterisks as in (A). Arrowheads, ring of tumor cells undergoing apoptosis. (**C**) Tumors harvested 72 hours after treatment with αvβ3-NP/Raf(–) (left and center panels) or control (right panel) were stained with hematoxylin and eosin. Necrotic tissues are denoted by N. Bar, 50 μm in left panel; 100 μm in center and right panels.

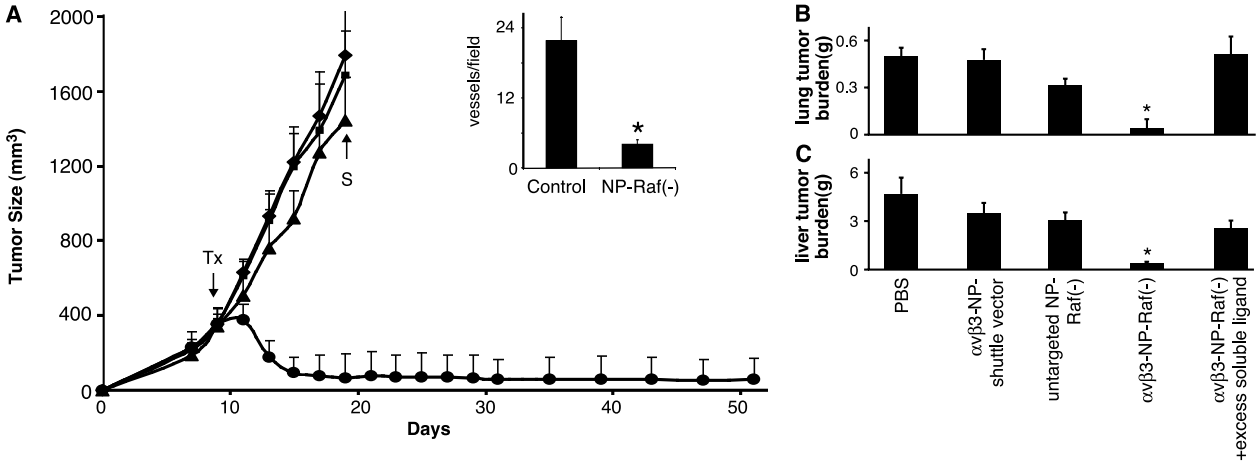

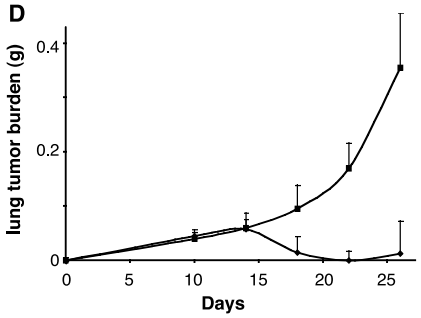

Fig. 4. Delivery of mutant *Raf* to tumor vessels inhibits angiogenesis, causing regression of established tumors. (**A**) Athymic WEHI mice subcutaneously implanted with M21-L melanoma cells were allowed to form tumors ~400 mm^3 in size and were then intravenously injected with αvβ3-NP/Raf(–) as in Fig. 3. Tx, start of treatment; S, killing of animals because of large tumor burden. (◆), PBS control; (■), αvβ3-NP-shuttle vector; (●), αvβ3-NP/Raf(–); (▲), αvβ3-NP/Raf(–) plus excess soluble αvβ3 ligand. Each point represents the mean ± SE of six replicates. (**Inset**) Tumors from the PBS control and from the αvβ3-NP/Raf(–) group were sectioned and stained with an antibody to VE-cadherin so that blood vessels could be counted in a 200× microscopic field. Each bar represents the mean ± SD of five replicates. (**B** to **D**) Pulmonary or hepatic metastases of αvβ3-negative, CT-26 colon carcinoma cells were formed in Balb/C mice by intravenous or splenic injection, respectively (*19*). Metastatic tumors were allowed to grow for 10 days before mice were injected i.v. on days 10 and 17. Organs were harvested on day 24 [(B) and (C)] or at indicated time points (D), weighed [(B) to (D)] (*23*), and photographed (*13*). (D) Each bar represents the mean of ± SD of six to eight mice. (Asterisk, $P < 0.05$).

apoptosis of the angiogenic endothelium. The fact that M21-L tumors lack αvβ3 and are not transduced by αvβ3-NP suggests that the antitumor effect is based on the antiangiogenic effects, not a direct effect on the tumor.

We next examined whether this therapy was effective against established syngeneic pulmonary and hepatic metastases of colon carcinoma. We injected murine CT-26 carcinoma cells either i.v. or intrasplenically into Balb/c mice. This experimental procedure typically results in the formation of lung or liver metastases, respectively, within four days (*19*). However, in our study, the pulmonary or hepatic metastases were established for 10 days before treatment with the NP/gene complexes to ensure that all animals contained actively growing lung or liver tumors. Control mice treated with PBS, αvβ3-NP complexed to a control vector, or nt-NP/Raf(–) showed extensive tumor burden in the lung or liver (Fig. 4, B and C) (*13*). In contrast, mice treated with αvβ3-NP/Raf(–) displayed little or no visible tumor metastasis (Fig. 4, B and C) (*13*), as demonstrated by a significant reduction in wet lung or liver weight (Fig. 4, C and D). Mice injected with αvβ3-NP/Raf(–) and a 20-fold molar excess of soluble targeting ligand had a tumor burden similar to that in control mice, demonstrating that this response is αvβ3-specific (Fig. 4, B and C). In a parallel study in which mice were killed and tumor volume was established during the course of the experiment, αvβ3-NP/Raf(–) was shown to cause regression of pulmonary metastases (Fig. 4D).

In summary, we have shown that pronounced tumor regressions can be achieved in mice by systemic delivery of an antiangiogenic gene that is targeted to the tumor vasculature. Several components of this strategy likely contribute to its pronounced antitumor activity, and these may be useful for similar treatments in humans. First, the NP used in this study has a multivalent targeting of integrin αvβ3 that selectively delivers genes to angiogenic blood vessels. A similar particle containing gadolinium and the αvβ3-targeting antibody, LM609, has been used successfully to image angiogenic blood vessels in tumor-bearing rabbits (*2*). Second, the mutant *Raf-1* gene, when delivered to these tissues, influences the signaling cascades of two prominent angiogenic growth factors, bFGF and VEGF (*13*). The robust proapoptotic activity of this gene is consistent with previous studies that have shown a role for *Raf-1* in promoting cell survival (*17*). Lastly, because NPs are less immunogenic than viral vectors, it may be feasible to deliver therapeutic genes repeatedly to angiogenic blood vessels for sustained treatment of diseases that depend on angiogenesis and vascular remodeling.

References and Notes

1. W. Arap, R. Pasqualini, E. Ruoslahti, *Science* **279**, 377 (1998).
2. D. A. Sipkins *et al.*, *Nature Med.* **4**, 623 (1998).
3. P. Blezinger *et al.*, *Nature Biotechnol.* **17**, 343 (1999).
4. Y. Wang *et al.*, *Nature Med.* **3**, 887 (1997).
5. S. Takeshita *et al.*, *Lab. Investig.* **75**, 487 (1996).
6. D. W. Losordo *et al.*, *Circulation* **98**, 2800 (1998).
7. G. D. Yancopoulos, M. Klagsbrun, J. Folkman, *Cell* **93**, 661 (1998).
8. B. P. Eliceiri, D. A. Cheresh, *Curr. Opin. Cell Biol.* **13**, 563 (2001).
9. P. C. Brooks *et al.*, *Cell* **79**, 1157 (1994).
10. A. Berinstein, M. Roivainen, T. Hovi, P. W. Mason, B. Baxt, *J. Virol.* **69**, 2664 (1995).
11. C. A. Guerrero *et al.*, *Proc. Natl. Acad. Sci. U.S.A.* **97**, 14644 (2000).
12. T. J. Wickham, P. Mathias, D. A. Cheresh, G. R. Nemerow, *Cell* **73**, 309 (1993).
13. Further characterization of the nanoparticle and details of its synthesis are available as supporting material at *Science* Online.
14. B. Felding-Habermann, B. M. Mueller, C. A. Romerdahl, D. A. Cheresh, *J. Clin. Investig.* **89**, 2018 (1992).
15. B. P. Eliceiri, R. Klemke, S. Stromblad, D. A. Cheresh, *J. Cell Biol.* **140**, 1255 (1998).
16. G. Heidecker *et al.*, *Mol. Cell. Biol.* **10**, 2503 (1990).
17. M. Huser *et al.*, *EMBO J.* **20**, 1940 (2001).
18. C. P. Carron *et al.*, *Cancer Res.* **58**, 1930 (1998).
19. R. Xiang *et al.*, *Cancer Res.* **57**, 4948 (1997).
20. M. E. Duggan *et al.*, *J. Med. Chem.* **43**, 3736 (2000).
21. Cells were exposed for 6 hours to NP electrostatically coupled to 25 μg of plasmid encoding GFP, washed with PBS, and grown in complete media. After 24 hours, cells were counterstained with 4′,6′-diamidino-2-phenylindole and fixed; GFP-expressing cells were enumerated by counting random microscopic fields. Each bar represents the mean ± SD of eight replicates.
22. FLAG-specific antibody was obtained from Zymed (South San Francisco, CA) and VE-cadherin from Santa Cruz Biotechnologies (Santa Cruz, CA). TUNEL staining was performed with the use of the Apoptag kit from Oncor (Gaithersburg, MD), and luciferase assays were performed with the use of the Luciferase assay kit from Promega (Madison, WI).
23. Weight due to tumor burden was calculated by subtracting the normal wet organ weight from each tumor-bearing organ.

24. We thank K. Spencer for assistance with immunofluorescent images and N. Alexander for assistance with vector preparation. Supported by a grant from Merck KGAa, the Lucas Foundation, the Phil Allen trust, and NIH P41 RR09784. S. Guccione is a National Cancer Institute fellow supported by NIH T32 CA09696 and CA50286. Patents are pending on αvβ3-NP and the use of ATP$^{\mu}$-Raf as antiangiogenic agents. This is TSRI manuscript number 14947-IMM.

Supporting Online Material

www.sciencemag.org/cgi/content/full/296/5577/2404/DC1

Materials and Methods

Figs. S1 to S3

24 January 2002; accepted 21 May 2002

Ongoing Modification of Mediterranean Pleistocene Sapropels Mediated by Prokaryotes

Marco J. L. Coolen,[1,2] Heribert Cypionka,[1] Andrea M. Sass,[1] Henrik Sass,[1] Jörg Overmann[1,3]*

Late Pleistocene organic-rich sediments (sapropels) from the eastern Mediterranean Sea harbor unknown, metabolically active chemoorganotrophic prokaryotes. As compared to the carbon-lean intermediate layers, sapropels exhibit elevated cell numbers, increased activities of hydrolytic exoenzymes, and increased anaerobic glucose degradation rates, suggesting that microbial carbon substrates originate from sapropel layers up to 217,000 years old. 16*S* ribosomal RNA gene analyses revealed that as-yet-uncultured green nonsulfur bacteria constitute up to 70% of the total microbial biomass. Crenarchaeota constitute a smaller fraction (on average, 16%). A slow but significant turnover of glucose could be detected. Apparently, sapropels are still altered by the metabolic activity of green nonsulfur bacteria and crenarchaeota.

Deep-sea sediments of the eastern Mediterranean are characterized by the cyclic occurrence of dark sediment layers, called sapropels. Sapropels differ from most other subsurface environments in that they contain high concentrations of total organic carbon (2 to 30.5% dry weight) (*1*), consisting mainly of dark brown amorphous, highly refractory kerogen (*2*). They are embedded in hemipelagic carbonate oozes that are poor in organic carbon (<0.5 weight percent) (*3*) and are likely to represent Pleistocene analogs of the widespread Mesozoic black shales (*4*). The presence of iso and anteiso fatty acids and of β-hydroxy fatty acids in the sapropels points toward a bacterial contribution to the organic matter (*5*). Because large numbers of bacteria

[1]Paleomicrobiology Group, Institute for Chemistry and Biology of the Marine Environment, University of Oldenburg, Post Office Box 2503, D-26111 Oldenburg, Germany. [2]Royal Netherlands Institute for Sea Research, Department of Biogeochemistry and Toxicology, Landsdiep 4, 1797 SZ, Den Hoorn, Netherlands. [3]Institute for Genetics and Microbiology, University of Munich, Maria-Ward-Strasse 1a, D-80638 München, Germany.

*To whom correspondence should be addressed. E-mail: j.overmann@LRZ.uni-muenchen.de

ERRATUM

post date 11 OCTOBER 2002

REPORTS: "Tumor regression by targeted gene delivery to the neovasculature" by J. D. Hood *et al.* (28 June 2002, p. 2404). The following text should have appeared in the acknowledgments in reference (*24*). "We would like to thank S. Narasimhan Danthi at Targesome for his contribution to synthesis of the targeting lipid used in the construction of the nanoparticle described in these studies. In addition, we want to thank Targesome for providing the trivalent lipid-integrin antagonist 1 described in Fig. 1 and used in these studies."

Tumor Regression by Targeted Gene Delivery to the Neovasculature

John D. Hood, Mark Bednarski, Ricardo Frausto, Samira Guccione, Ralph A. Reisfeld, Rong Xiang and David A. Cheresh

Science **296** (5577), 2404-2407.
DOI: 10.1126/science.1070200